

Energy-efficient motion camouflage in three dimensions

N.E. Carey, M.V. Srinivasan

Abstract

Recent observations suggest that one insect may camouflage its own motion whilst tracking another. Here we present a strategy by which one agent can efficiently track and intercept another agent, whilst camouflaging its own motion and minimizing its energy consumption.

1 Introduction

The past decade has witnessed increasing interest in a phenomenon known as ‘motion camouflage’ – a term coined by Srinivasan and Davey (1996) to explain a class of interactive manoeuvres in hoverflies, observed by Collett and Land (1975). Srinivasan and Davey noted that, in certain circumstances, one hoverfly (A) would ‘shadow’ another hoverfly (B) by moving in such a way as to mimic the optic flow that would be produced by a stationary object in B’s retina, thus ‘camouflaging’ its own motion and escaping detection. As illustrated in Fig. 1, A (the shadower) tracks B (the shadowee) by moving in such a way that A always remains on a straight line connecting B with a fixed, stationary point (S) in the environment. If A moves in this way, the trajectory of its image will be indistinguishable from the trajectory produced by a stationary object located at S. The lines connecting the shadowee to the fixed point are termed ‘camouflage constraint lines’ (CCLs), because successive positions of the shadower are constrained to lie on these lines if motion camouflage is to be maintained. This analysis assumes that A is small enough or sufficiently far away from B that it appears as a point object in B’s retina, and thus does not create any noticeable image expansion or contraction.

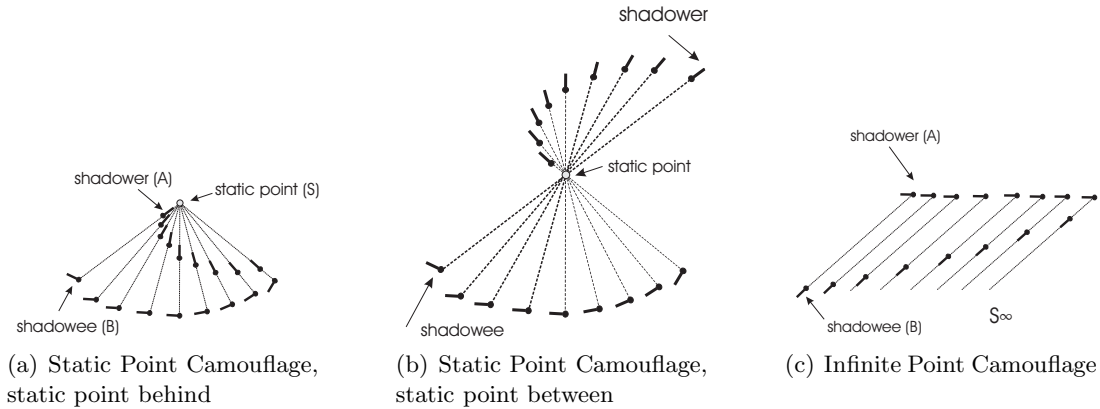


Figure 1: Depiction of the primary types of motion camouflage

How should an animal move if it is to minimize energy consumption (for example), or interception time, whilst camouflaging its motion? In general, such trajectories can be calculated only if the trajectory of the shadowee is known, or can be reliably predicted [5], [14]. Anderson and McOwen [1] tackled this limitation by training artificial neural networks to control simulated shadowers. Their design used a control system formed from three separate neural networks, and calculated a control command based upon the distance from the chosen static point, the direction required for camouflage maintenance, and

the line-of-sight error angle to the target. However the usual limitations of neural network solutions still applied. An exploration of the entire state-space was necessary prior to commencement of the learning period for the networks. The resulting controller was tailored to a specific type of shadowee trajectory, and lost performance quality when encountering unexpected varieties of motion.

A more traditional approach is to create a linear quadratic feedback controller to govern the behaviour of the shadowee [5]. The deviation of the shadower’s trajectory from that dictated by the CCLs (in two dimensions) is used in conjunction with a weighted penalty on control action to create a cost function that results in a stable feedback controller. However, without a limit placed on the maximum control effort that could be requested, the required control acceleration can be very large, especially if a shadowee executes a trajectory that is highly non-linear. And placing a realistic cap on the control commands compromises the accuracy of the resulting trajectory. Moreover, such a controller is a) not biologically realistic and b) designed to perform on a predictable shadowee path. Erratic or non-predictable paths are very calculation-intensive, as the solution has to be recalculated for each movement made by the shadowee.

Reddy et al. explored dynamic models in both two [7] and three [13] dimensions, restricting the case to motion camouflage where the shadower emulates a fixed point that is infinitely far away. Their research was inspired by insect-capture behaviour in echo-locating bats. They modelled the shadower and shadowee as points subject to curvature control, rather than speed control (as is more traditional). They derived a feedback control law for motion camouflage using neural networks, which they called ‘motion camouflage proportional guidance’ [7], and then extended this planar guidance law to three dimensions, describing the particle trajectories using natural Frenet frames [7], [8].

Motivated by the work of [14] and [11], Glendinning [12] developed an explicit mathematical description of the geometry governing a motion camouflaged interaction. While an infinite number of potential camouflage paths exist for any given prey trajectory, his analysis allows us to prescribe further constraints on the behaviour of the shadower, that can give rise to a unique solution.

Here we present a method for devising 3-dimensional trajectories which not only achieve perfect motion camouflage but do so in an energy-efficient manner. This approach will be useful in the design of energy-optimal controllers.

2 Background

Glendinning [12] characterized motion camouflaged paths mathematically in the following way. In 3-D Cartesian space, let $\mathbf{r}_D(t)$ and $\mathbf{r}_T(t)$ be the vectors representing the time-varying paths of the pursuer and the target, respectively, and let \mathbf{r}_P be the vector that represents the position of the fixed point. The camouflage constraint then requires that, at all times t ,

$$\mathbf{r}_D(t) = \mathbf{r}_D(0) + k(t)(\mathbf{r}_T(t) - \mathbf{r}_P),$$

ie

$$\mathbf{r}_P - \mathbf{r}_D(t) = k(t)(\mathbf{r}_P - \mathbf{r}_T(t)) \quad \forall \quad t > 0 \quad (1)$$

where $\{k(t) | -\infty < k(t) \leq 1\}$ is a continuous time-varying scalar function. Positive $k(t)$ corresponds to figure 1(a), negative $k(t)$ corresponds to figure 1(b). (Infinite point camouflage, as in figure 1(c), requires a slightly different formulation, as discussed in section 3.2).

This equation is simply a quantitative statement of the requirement that the pursuer should always be located on the straight line connecting the target to the fixed point. k may be thought of as representing the ratio in range between the shadowee and shadower, with reference to the static point P , at any time t . Since $k(t)$ can be any (bounded) continuous function, there are infinitely many trajectories that will satisfy the requirement of motion camouflage. The task of the analyst, then, is to determine constraints which lead to a unique path description. For example, we may require interception to occur in minimum time, or, as in this paper, with minimum expenditure of energy.

3 Procedure

3.1 Camouflage with a non-infinite static point

We assume the function $k(t)$ to be twice differentiable, and that the initial conditions of the system are known. As is traditional, we ignore any gravitational effects. We then take an energy minimization approach to finding an optimal path, using Lagrangian mechanics. In classical and quantum mechanics, equations of motion are derived from what is termed the 'principle of least action'. 'Action' is a quantity which has dimensions of energy integrated over time. The energy in question is expressed by an equation known as the Lagrangian, and is generally taken as being the kinetic energy of the system minus its potential energy. Let the transpose of a vector \mathbf{x} be represented as \mathbf{x}' , then assuming a particle of unit mass, the Lagrangian for the motion-camouflaged system can be written as

$$\mathcal{L} = KE - PE = \frac{1}{2} \dot{\mathbf{r}}_D' \dot{\mathbf{r}}_D \quad (2)$$

ie kinetic energy minus potential energy [9] (note that since we are ignoring any gravitational force, the potential energy term can be neglected). By solving the Euler-Lagrange equations for such a system, we can use Hamilton's Principle of Least Action [2] to find the path the particle will take if no other forces are acting on it besides those required to keep the motion camouflaged. To accomplish this, we set the system cost to be the integral of the Lagrangian,

$$J = \frac{1}{2} \int_{t_0}^t \dot{\mathbf{r}}_D' \dot{\mathbf{r}}_D dt \quad (3)$$

Differentiating equation (1) with respect to time, we obtain

$$-\dot{\mathbf{r}}_D(t) = \dot{k}(t)(\mathbf{r}_P - \mathbf{r}_T(t)) - k(t)\dot{\mathbf{r}}_T(t) \quad (4)$$

Since $k(t)$ parameterizes the path of the shadower, finding an appropriate stationary value for the energy curve

$$\frac{1}{2} \int_{t_0}^t \dot{\mathbf{r}}_D(t)' \dot{\mathbf{r}}_D(t) dt \quad (5)$$

is equivalent to finding the function $k(t)$ such that the quantity

$$\frac{1}{2} \int_{t_0}^t \left[k(t)\dot{\mathbf{r}}_T(t) - \dot{k}(t)(\mathbf{r}_P - \mathbf{r}_T(t)) \right]' \left[k(t)\dot{\mathbf{r}}_T(t) - \dot{k}(t)(\mathbf{r}_P - \mathbf{r}_T(t)) \right] dt \quad (6)$$

is minimised. We do this by solving the Euler-Lagrange (E-L) equation [9]. With \mathcal{L} as before, the E-L equation for the system is

$$\frac{\partial \mathcal{L}}{\partial k} - \frac{d}{dt} \frac{\partial \mathcal{L}}{\partial \dot{k}} = 0. \quad (7)$$

Expanding this, we obtain a second-order differential equation in k :

$$\ddot{k} [(\mathbf{r}_P - \mathbf{r}_T)'(\mathbf{r}_P - \mathbf{r}_T)] + 2(-\dot{k} [\dot{\mathbf{r}}_T'(\mathbf{r}_P - \mathbf{r}_T)]) + k [-\dot{\mathbf{r}}_T'(\mathbf{r}_P - \mathbf{r}_T)] = 0. \quad (8)$$

Setting $(\mathbf{r}_P - \mathbf{r}_T(t)) = \alpha(t)$, we can write (8) as:

$$\ddot{k}\alpha'\alpha + 2\dot{k}\dot{\alpha}'\alpha + k\ddot{\alpha}'\alpha = 0. \quad (9)$$

In other words,

$$\left(\frac{d^2}{dt^2} (k\alpha) \right) \cdot \alpha = 0, \quad (10)$$

hence we can state that $k(t)$ will satisfy the Lagrangian conditions when the acceleration of the pursuer is orthogonal to the line-of-sight vector between the pursuer and target.

This ODE does not have a general analytical solution, but it is amenable to numerical solution methods. Moreover, given further information about the target path, we can develop analytical solutions. In the following sections, we will primarily focus on the homogenous solution, which occurs when the target travels in a straight line at constant velocity, however some attention will be paid to other quantifiable target trajectories.

3.2 Camouflage at Infinity

A similar method can be used to generate optimal paths with camouflage at infinity [14]. We again use a general formulation given by Glendinning [12]:

$$\mathbf{r}_T - \mathbf{r}_D = k(t)\mathbf{e} \quad (11)$$

where \mathbf{e} is a constant vector. For the sake of simplicity, we choose \mathbf{e} to correspond with the initial conditions, so

$$\mathbf{e} = \mathbf{r}_T(t_0) - \mathbf{r}_D(t_0). \quad (12)$$

Differentiating and applying the same cost function as before, we obtain the Lagrangian and develop a solution. Fortunately, the Euler-Lagrange equation for camouflage at infinity is solvable analytically, and we find the function $k(t)$ has a general solution of the form

$$k\mathbf{e}^T\mathbf{e} = \mathbf{r}_T^T\mathbf{e} + c_1t + c_2 \quad (13)$$

for some constants of integration c_1, c_2 .

4 Examples of optimal motion camouflage equations

With more information about the target trajectory, we can simplify the problem and discover an analytic solution. In this section, we present a few examples of optimal motion camouflage against targets with various dynamic characteristics.

4.1 Camouflage against a target moving at constant velocity

We begin by assuming that the target moves in a straight line at constant velocity, ie $\ddot{\mathbf{r}}_T = 0$. Solving equation (10) is then equivalent to solving the second-order homogenous differential equation

$$\frac{d^2}{dt^2}(k\|\alpha\|) = 0. \quad (14)$$

Equation 14 has a solution of the form

$$k\|\alpha\| = c_1t + c_2 \quad (15)$$

for some integration constants c_1, c_2 ; therefore

$$k(t) = \frac{c_1t + c_2}{\|\mathbf{r}_P - \mathbf{r}_T(t)\|}. \quad (16)$$

This represents the general solution for the optimum form of $k(t)$ which satisfies the specified constraints. Clearly it encompasses the trivial solution, $k(t) = 0 \forall t$. Explicit values for the constants depend on the initial conditions, so it is evident that the solution is highly sensitive to the choice of starting position and velocity, as is often the case with variational problems [9]. The value of c_2 is found as follows: assuming the initial conditions of pursuer, target and fixed point are known. We allow $t_0 = 0$, then $k_0 = k(t_0) = k(0)$ is known. By substituting into 16, we solve for c_2 ,

$$c_2 = k_0(\|\mathbf{r}_P - \mathbf{r}_T(0)\|). \quad (17)$$

For an engagement that ends in an interception, c_1 can be similarly found from the desired terminal conditions, a procedure outlined later. However for an open-ended interaction, a suitable value for the constant c_1 can still be established from the first-order initial conditions. Differentiating (15) gives us

$$\dot{k} = \frac{c_1}{\|\mathbf{r}_P - \mathbf{r}_T\|} + k \frac{\dot{\mathbf{r}}_T'(\mathbf{r}_P - \mathbf{r}_T)}{\|\mathbf{r}_P - \mathbf{r}_T\|^2} \quad (18)$$

therefore by defining the initial condition \dot{k}_0 , we obtain

$$c_1 = \dot{k}_0(\|\mathbf{r}_P - \mathbf{r}_T(t_0)\|) - k_0 \frac{\dot{\mathbf{r}}_T(t_0)'(\mathbf{r}_P - \mathbf{r}_T(t_0))}{\|\mathbf{r}_P - \mathbf{r}_T(t_0)\|}.$$

A positive value of \dot{k}_0 generates a trajectory with a pursuit characteristic, a negative value gives an escape path. Different engagements are illustrated below. Figure 2(a) shows an example involving a constant-velocity target. A positive value is used for k , which results in a pursuit scenario. Figure 2(b) shows a trajectory with the same starting conditions, but in which k is negative, so that the shadower escapes from the shadowee.

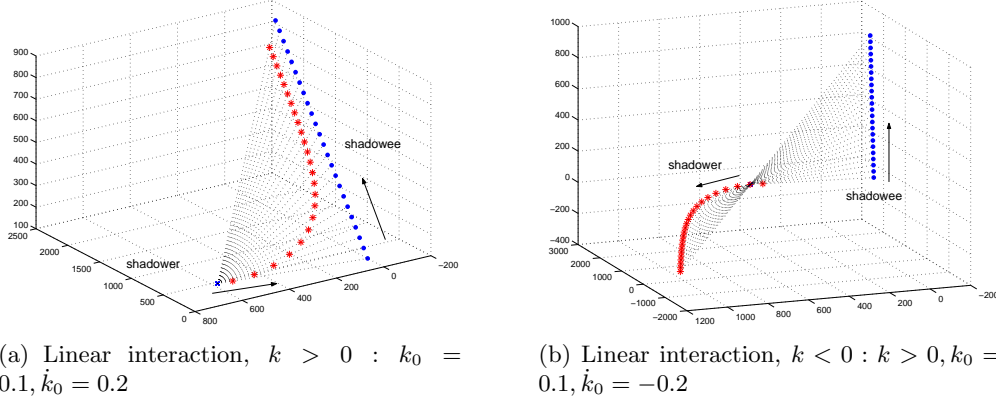


Figure 2: Optimal solutions to linear trajectories

To demonstrate the energy efficiency of these paths, we consider two agents with the same starting position and velocity, camouflaging themselves against a shadowee moving along a prescribed straight trajectory. One agent uses the low-energy path as derived above, while the other moves in a straight line to the interception point (whilst still maintaining camouflage). Figure 3 shows the paths taken. (For simplicity, we look at only two dimensions in this instance).

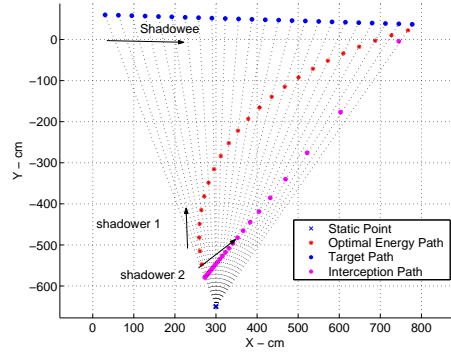


Figure 3: Comparison between a straight interception trajectory and an energy optimal trajectory. Initial conditions, in cm, are as follows: $X_T(0) = [30, 60]$, $V_T(0) = [650, -20]$, $X_D(0) = [300, -650]$, $V_D(0) = [9, 11]$

The initial velocity vector of the straight line path was set to point in the approximate direction of the interception point of the optimal trajectory, as to enable a meaningful comparison. The forward velocity of both pursuers at the beginning of the interaction is 14 cm/s. The final speed required for the straight trajectory to still be camouflaged at the interception point is 1.14×10^3 cm/s, whereas that required for the optimal energy path is very much lower, 187.8 cm/s. Given these initial conditions,

then, to pursue a target along a straight line while remaining camouflaged, a shadower must expend more than 40 times the energy that would be required by a low-energy pursuit curve.

As alluded to previously, if it is desired to intercept the shadower within a predetermined time (a so-called 'finite horizon' capture), or indeed if another geometric condition is to be met, then we can determine the necessary constant c_1 from the end boundary conditions. In the case of capture in some finite time t_f , we say $k(t_f) = 1$, so substituting this condition and equation 17 into equation 16, we can write:

$$c_1 = \frac{1}{t_f} [\|\mathbf{r}_P - \mathbf{r}_T(t_f)\| - k_0 \|\mathbf{r}_P - \mathbf{r}_T(t_0)\|]. \quad (19)$$

Figure 4 demonstrates a finite horizon capture path.

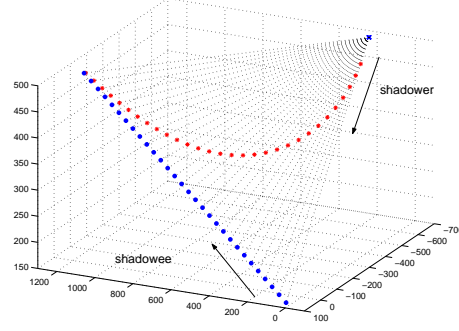


Figure 4: Capture trajectory for a shadower with initial conditions $k_0 = 0.1$, $\dot{k}_0 = 0.2$, static point at $\mathbf{r}_P = [200, -650, 500]$. Shadowee initial conditions $\mathbf{r}_T(0) = [30, 60, 150]$, constant velocity $\mathbf{r}_T = [200, -20, 60]$. Capture horizon is 12s (CCLs shown here every 0.4s).

A similar method can be used to find a trajectory for camouflage at infinity against a target moving at constant velocity. Recall equation 13. We can again find the constants c_1 and c_2 from the initial position and velocity conditions. Alternatively, for a capture trajectory, we can determine the optimal c_1 for a given final time from the terminal boundary conditions, so

$$c_1 = \frac{1}{t_f} (k(t_f)\mathbf{e}^T \mathbf{e} - \mathbf{r}_T^T(t_f)\mathbf{e} - c_2). \quad (20)$$

For a capture trajectory, $k(t_f) = 0$, and this is demonstrated in Figure 5. For tracking at a constant distance $d = \|\mathbf{r}_{T_0} - \mathbf{r}_{D_0}\| = \|\mathbf{e}\|$, we set $k(t_0) = k(t) = k(t_f) = 1$. An example of the latter tracking result can be seen in Figure 6.

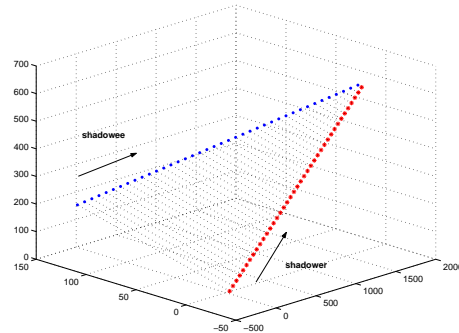


Figure 5: Capture using camouflage at infinity. Initial conditions and velocity of the shadowee are $\mathbf{r}_T(t_0) = [-301, 501, 150]$, $\mathbf{v}_T(t_0) = [200, -20, 60]$. Starting point of shadower is at $[0, 0, 0]$.

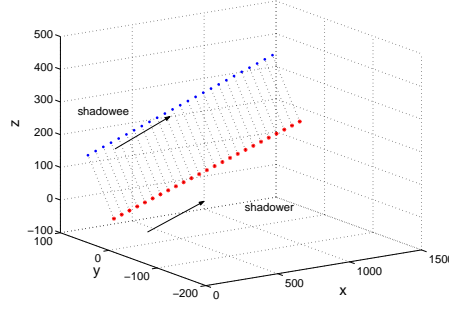


Figure 6: Tracking at a constant distance. Initial conditions and velocity of the shadowee are identical to Figure 4. Starting point of shadower is at $[0, 0, 0]$.

4.2 Camouflaging against a target following a quasi-3D guidance law

In *conspicuous* two-body guidance, it may be surmised that both participants have similar capabilities and are using similar guidance techniques. In such a scenario, it is unlikely that one participant will maintain a constant linear (or angular) velocity while the other does not, so the conditions on target dynamics assumed in the previous examples may not be useful. However in a *conspicuous* situation, we may be able to use the similarity of the participants to come up with some other constraint on the target motion. One such example follows here.

Recall that our main result in equation 10 shows that the pursuer's acceleration under Lagrangian camouflage conditions will be orthogonal to the line-of-sight vector between pursuer and target. An interaction of this nature will produce a relative motion vector that lies in a plane. Bodies with trajectories satisfying this condition are said to be moving in a 'quasi-3dimensional' manner [15]. Certain commonly used guidance laws which result in quasi-3D motion have as their defining characteristic a relative acceleration of zero along the radial axis between shadowee and shadower, as does motion camouflage. We examine a situation where the shadower, D , is following a motion camouflaged path, and the shadowee, T , is following a quasi-3D guidance law - in other words, the shadower and shadowee are using similar (but possibly non-identical) guidance strategies, both accelerating in a direction orthogonal to the line-of-sight. Using this information, we can make a general statement about the function $k(t)$ under these conditions.

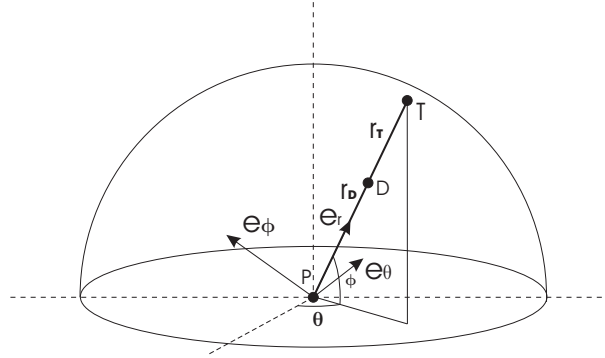


Figure 7: Geometry of motion camouflage in three dimensions in a spherical reference frame, with origin at the static point.

We examine a camouflaged engagement in a spherical reference frame (Figure 7). The origin is fixed at the static point of the engagement, and the co-ordinates of the pursuer and target can be written (r_D, θ_D, ϕ_D) and (r_T, θ_T, ϕ_T) respectively. It is straightforward to show that under motion

camouflage conditions, $\theta_D = \theta_T = \theta$, $\phi_D = \phi_T = \phi$. Hence we can define an orthogonal set of unit vectors ($\mathbf{e}_r, \mathbf{e}_\theta, \mathbf{e}_\phi$) along the co-ordinate axes, as in Figure 7.

The displacement and velocity of the pursuer in this reference frame can be written

$$\begin{aligned}\mathbf{r}_D &= r_D \mathbf{e}_r \\ \dot{\mathbf{r}}_D &= \dot{r}_D \mathbf{e}_r + r_D \dot{\theta} \cos \phi \mathbf{e}_\theta + r_D \dot{\phi} \mathbf{e}_\phi\end{aligned}\quad (21)$$

hence the acceleration components along the co-ordinate axes are

$$a_{D_r} = \ddot{r}_D - r_D \dot{\phi}^2 - r_D \dot{\theta}^2 \cos^2 \phi \quad (22a)$$

$$a_{D_\theta} = r_D \ddot{\theta} \cos \phi + 2\dot{r}_D \dot{\theta} \cos \phi - 2r_D \dot{\phi} \dot{\theta} \sin \phi \quad (22b)$$

$$a_{D_\phi} = r_D \ddot{\phi} + 2\dot{r}_D \dot{\phi} + r_D \dot{\theta}^2 \cos \phi \sin \phi. \quad (22c)$$

According to equation (10), the acceleration of the pursuer D is entirely orthogonal to the line-of-sight vector \mathbf{e}_r , or in other words, the radial component of the acceleration is zero. Hence we can write

$$\ddot{r}_D - r_D(\dot{\theta}^2 \cos^2 \phi + \dot{\phi}^2) = 0.$$

Applying equation (1), we establish the following condition for $k(t)$:

$$\frac{d^2}{dt^2}(kr_T) = r_T(\dot{\theta}^2 \cos^2 \phi + \dot{\phi}^2). \quad (23)$$

The angular velocity of D is found in the following way:

$$\boldsymbol{\Omega} = \frac{\mathbf{r}_D \times \dot{\mathbf{r}}_D}{r_D^2} = -\dot{\phi} \mathbf{e}_\theta + \dot{\theta} \cos \phi \mathbf{e}_\phi, \quad (24)$$

hence we can replace (23) with the following general equation:

$$\frac{d^2}{dt^2}(kr_T) = r_T \Omega^2. \quad (25)$$

Let $\mathbf{r} = \mathbf{r}_T - \mathbf{r}_D$. If the shadowee is using a quasi-3D guidance law to react to the shadower, then the following holds true [15]:

$$\frac{d^2}{dt^2}r = r\Omega^2 \quad (26)$$

We can write the left-hand side of this equation in terms of r_T, k :

$$\begin{aligned}\ddot{r} &= \frac{d^2}{dt^2}(r_T(1-k)) \\ &= \ddot{r}_T - (\ddot{k}r_T + 2\dot{k}\dot{r}_T + k\ddot{r}_T) \\ &= \frac{d^2}{dt^2}(r_T) - \frac{d^2}{dt^2}(kr_T).\end{aligned}\quad (27)$$

Doing the same to the right-hand side, we find

$$\frac{d^2}{dt^2}(r_T) - \frac{d^2}{dt^2}(kr_T) = r_T \Omega^2 - (kr_T) \Omega^2. \quad (28)$$

Recall the general equation described in (25). We can rearrange this to find a differential equation in k, r_T to describe Ω :

$$\Omega^2 = \frac{1}{kr_T} \frac{d^2}{dt^2}(kr_T) \quad (29)$$

Substituting into (28) and expanding, we find that k satisfies the following differential equation:

$$\ddot{k}r_T + 2\dot{k}\dot{r}_T = 0$$

which has a solution

$$k(t) = c_1 + c_2 \int_{t_0}^t \frac{1}{r_T(t)^2} dt. \quad (30)$$

The exact form of $k(t)$ and the constants c_1, c_2 depend on the precise formulation of the guidance law being used by the shadowee and the initial conditions of the engagement. An example of two-body guidance using a specific quasi-3D guidance law is given in section 5.2.

5 Possible Applications

In order to demonstrate a possible use for these optimal path equations, we consider what kind of guidance system may be easily modified to produce trajectories which satisfy the above conditions. A common tracking strategy which has been observed in insects such as blowflies and houseflies [4], [10], is for the pursuer to apply an acceleration proportional to the relative angular velocity between the pursuer and target. This type of guidance is conventionally known as proportional navigation (PN), and as well as being observed in nature, has been used for many years in autonomous and independently guided tracking systems. Motion camouflage is a natural candidate for a modified PN guidance law [7], since the relative angular position is a key variable when it comes to defining and controlling for motion camouflage.

Consider the problem of static point motion camouflage in two dimensions. We use a polar reference frame, as in section 4.2, however for simplicity we will restrict ourselves to two dimensions. This coordinate system can be described by $(\mathbf{e}_r, \mathbf{e}_\theta)$, where \mathbf{e}_r is a unit vector along the line-of-sight (LOS) between agents D and T , and \mathbf{e}_θ is a unit vector orthogonal to \mathbf{e}_r .

Given equations (26) and (10) we can write the acceleration of the shadower D as

$$a_D = a_{D_\theta} = (kr_T)\ddot{\theta} + 2\frac{d}{dt}(kr_T)\dot{\theta}.$$

It is straightforward to see that the above is equivalent to

$$a_D = ka_T + 2kr_T\dot{\theta}. \quad (31)$$

This is a form of augmented PN guidance, which we term MCPN, and depending on the value of a_T , this augmented equation may reduce further to a simple PN function. For example, if the shadowee is moving with a constant velocity, we can write equation (31) in terms of the relative distance and line of sight velocity,

$$\begin{aligned} a_D &= 2\frac{\dot{kr}}{1-k}\dot{\theta} \\ &= \Gamma r\dot{\theta} \end{aligned} \quad (32)$$

where Γ is a variable gain function depending on the ratio (k) of the distances of the shadower and shadowee from the static point.

5.1 MCPN Guidance against a target moving at constant velocity

We assume an oblivious target moving at constant velocity. The relevant guidance law is described in equation 32. Figure 8(b) shows the camouflage path achieved using a PN-guided pursuer following a motion camouflaged path under locally energy-minimal conditions (MCPN), and the radial and angular acceleration required.

5.2 MCPN guidance against a reactive guided target

Previously (§4.2) we discussed a conspecific pursuit scenario. There, we derived a motion camouflage equation that may be used against a reactive shadowee which is simultaneously tracking the shadower. This may possibly be of use to robotics researchers or autonomous agents - it will almost certainly give us some insight into the flight patterns seen in insects known to use motion camouflage. Hence we now develop a guidance law that may be used to maintain camouflage against a similarly capable manoeuvring target, provided that some rudimentary facts about the target dynamics are known.

Suppose the shadowee T has a non-constant velocity, and in fact is also tracking the pursuer, using a known guidance law. Let the shadowee be using a quasi-3D proportional guidance law known as True Proportional Navigation (TPN), which takes the form

$$a_T = \lambda \dot{r}_0 \dot{\theta}. \quad (33)$$

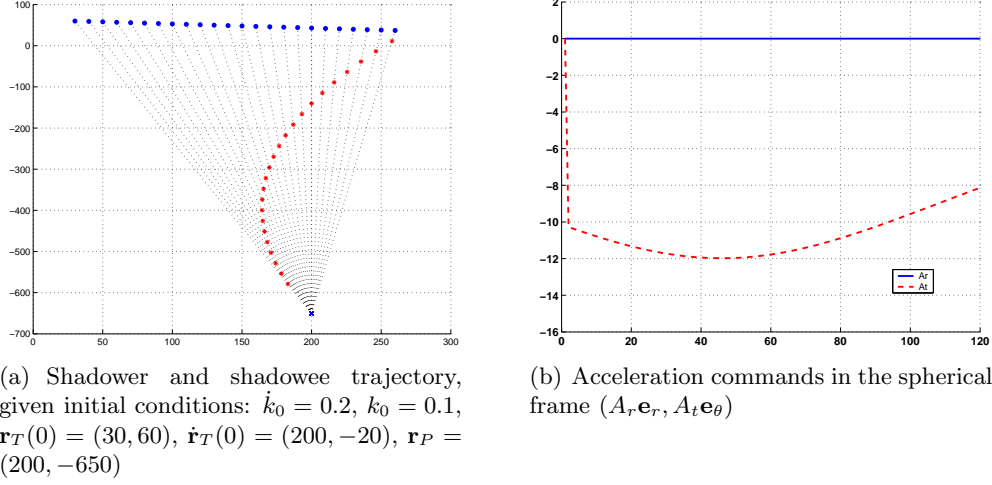


Figure 8: Motion Camouflage path for a non-maneuvering target using PN-derived acceleration commands. Note that in figure (b), $A_r = 0$, as expected.

In this formulation, λ is a gain constant, \dot{r}_0 is the initial range between the shadower and shadowee, and θ is the line-of-sight vector between shadower and shadowee (from the shadowee's perspective).

Recall that according to Yang and Yang [15], with a quasi-3D guidance law, the relative radial acceleration $a_{R_r} = 0$. From (10) we know $a_{D_r} = 0$, hence we can state that $a_{T_r} = 0$. Therefore for a shadowee using TPN against a motion camouflaged shadower, the following two equations hold:

$$\ddot{r}_T = r_T \dot{\theta}^2 \quad (34a)$$

$$a_T = r_T \ddot{\theta} + 2\dot{r}_T \dot{\theta} = \lambda \dot{r}_0 \dot{\theta} \quad (34b)$$

We make the following variable substitution [15]: let $V_r = \dot{r}_T$, $V_\theta = r_T \dot{\theta}$, then the equations in (34) become

$$\dot{V}_r - V_\theta \dot{\theta} = 0 \quad (35a)$$

$$\dot{V}_\theta + V_r \dot{\theta} = \lambda \dot{r}_0 \dot{\theta} \quad (35b)$$

We can change the independent variable t to θ and solve the above to find

$$V_r = A \cos(\theta + B) + \lambda \dot{r}_0 \quad (36)$$

$$V_\theta = -A \sin(\theta + B) \quad (37)$$

where A, B are constants (which can be found from initial conditions). From (37) and (30), $k(t)$ takes the following form:

$$k(t) = c_2 + c_1 \int_{t_0}^t \frac{-\dot{\theta}^2}{A^2 \sin^2(\theta + B)} dt \quad (38)$$

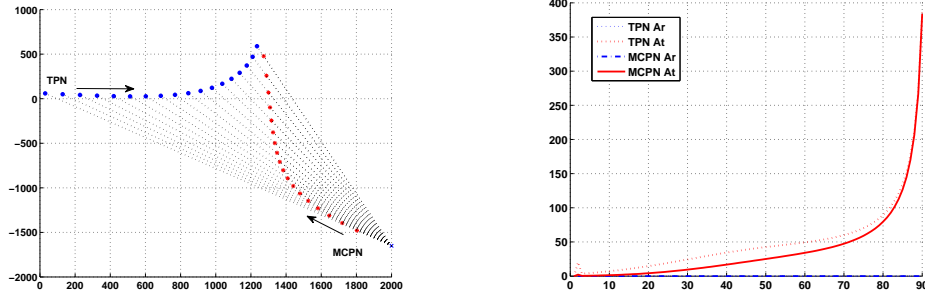
$$B = \arctan\left(\frac{r_{T_0} \dot{\theta}_0}{\lambda \dot{r}_0 - \dot{r}_{T_0}}\right) + \theta_0$$

$$A = \frac{\dot{r}_{T_0} - \lambda \dot{r}_0}{\cos(\theta_0 + B)} \quad (39)$$

which can be solved numerically. The shadower acceleration can be written

$$a_D = (\lambda k \dot{r}_0 + 2r \frac{\dot{k}}{1-k}) \dot{\theta} = \Gamma^* \dot{\theta}, \quad (40)$$

which again gives us a PN guidance law, this time with variable gain Γ^* . A guided shadower using a low-energy path derived with the above method against a guided target can be seen in Figure 9(a), and the desired accelerations of both target and pursuer are shown in Figure 9(b).



(a) The shadowee path is labelled 'TPN law', the shadower's path is labelled 'MCPN'. Initial conditions are: $\mathbf{r}_P = (2000 - 1650)$, $\mathbf{r}_T(0) = (30, 60)$, $\dot{\mathbf{r}}_T(0) = (200, -20)$.

(b) Acceleration commands in the respective body-centred spherical frame for both shadowee (TPN) and shadower (MCPN)

Figure 9: MCPN path against an active target using TPN guidance. (a) Pursuer and target trajectory, given $\dot{k}_0 = 0.08$, $k_0 = 0.1$ (b) Acceleration commands in the spherical frame for both pursuer and target ($A_r \mathbf{e}_r, A_t \mathbf{e}_\theta$). For both bodies, the radial acceleration is zero. As the endgame approaches, the acceleration of both shadowee and shadower increases, but over the course of the interaction the acceleration of the MCPN body is notably less than that of the TPN body.

It is hoped that by finding elegant and efficient means of mimicking pursuits and interactions observed in nature, we can gain insight into the guidance mechanisms used by insects and other animals. For example, research by Boeddeker, et al [4], and Land, et al [10], has found that insect pursuit systems can be modelled quite simply using a static first-order gain controller with only a few input variables readily available via the visual system. Similarly, Ghose, et al [6], show evidence that bats use an interception strategy commonly found in guided missiles to intercept prey. By combining these simple models with a guidance system that enables us to replicate gross characteristics of known flights, we can obtain a streamlined but fully controllable navigational system.

6 Conclusion

This study describes how energy-efficient strategies can be derived for tracking or shadowing moving objects whilst maintaining motion camouflage. A series of control strategies is presented for implementing energy-efficient motion camouflage under various conditions. The findings can be usefully applied to a variety of tracking situations, as well as provide insights into some of the behaviours exhibited by insects and animals. Our most important result was the discovery of a necessary orthogonal condition to the pursuer acceleration under an energy-optimal motion camouflage path.

This work was funded by an ANU Postgraduate Scholarship (to N.C.) and had partial support from the ARC Centre of Excellence in Vision Science (to M.S.). The authors would like to thank Jochen Zeil for discussion and advice and Alan Carey for an illuminating conversation.

References

- [1] Anderson, A. J. & McOwan, P. W. 2003 Model of a predatory stealth behaviour camouflaging motion. *Proc. R. Soc. Lond. B* **270**, 489-495

- [2] Bertsekas, D. P. 1996 Constrained Optimization and Lagrange Multiplier Methods, Athena, Massachusetts
- [3] Bishop, R. L. 1975 There is more than one way to frame a curve, *The American Mathematical Monthly*, **82**, 246-251,
- [4] Boeddeker, N., Kern, R. & Egelhaaf, M. 2003 Chasing a dummy target: smooth pursuit and velocity control in male blowflies. *Proc. R. Soc. B: Biological Sciences* **270** 1971-1978
- [5] Carey, N. E., Ford, J. J. & Chahl J. S. 2004 Biologically Inspired Guidance for Motion Camouflage *Proc. 5th Asian Control Conference* **3**, 1793-1799
- [6] Ghose K., Horiuchi T.K., Krishnaprasad P.S. & Moss C. F. 2006 Echolocating Bats Use a Nearly Time-Optimal Strategy to Intercept Prey. *PLoS Biol* 4(5): e108 doi:10.1371/journal.pbio.0040108
- [7] Justh, E. W. & Krishnaprasad, P. S. 2006 Steering laws for motion camouflage *Proc R Soc Lond A* **462** 3629-3643.
- [8] Justh, E. W. & Krishnaprasad, P. S. 2005, Natural frames and interacting particles in three dimensions *Proc. 44th IEEE Conf. Decision and Control*, 2841-2846, IEEE, New York
- [9] Milyutin, A.A. & Osmolovskii, N.P. 1998 Calculus of variations and optimal control, American Mathematical Society
- [10] Land, M.F. & Collett, T.S. 1974 Chasing behaviour of houseflies: *Fannia canicularis* *J. Comp. Physiol.* **89**, 331-57
- [11] Mizutani, A., Chahl, J.S. & Srinivasan, M.V. 2003 Motion Camouflage in Dragonflies, *Nature*, **423**, 604
- [12] Glendinning, P. 2004 The mathematics of motion camouflage. *Proc. R. Soc. Lond. B* **271**, 277-481
- [13] Reddy, P. V., Justh, E. W. & Krishnaprasad P. S. 2006 Motion camouflage in three dimensions, *Proc 45th IEEE Conf. Decision and Control*, 3327-3332, IEEE, New York. (also preprint at arXiv:math/0603176)
- [14] Srinivasan, M.V. & Davey, M. 1996 Strategies for active camouflage of motion. *Journal of Experimental Biology* **199**, 129-140
- [15] Yang, C.D. & Yang, C.C. 1997 A Unified Approach to Proportional Navigation, *IEEE Transactions on Aerospace and Electronic Systems* **33** Issue 2, 557-567